

Measurement of fast electron distribution using a flexible, high time resolution hard x-ray spectrometer

R. O'Connell, D. J. Den Hartog, and C. B. Forest
University of Wisconsin-Madison, Madison, Wisconsin 53706

R. W. Harvey
CompX, California

(Presented on 10 July 2002)

A 16 spatial channel hard x-ray (HXR) diagnostic using solid state CdZnTe detectors (active area 10 mm×10 mm×2 mm, 50 mm×20 mm×20 mm packaged) has recently been installed on the Madison Symmetric Torus (MST) reversed field pinch to measure the XR flux from ~10 to 300 keV. Rather than using conventional pulse height analysis, the shaped output pulses from the detector are digitized using 12-bit, 10 MHz ADCs. The resulting waveforms are then fitting with multiple Gaussians; this allows a fraction of normally discarded pile-up events to be recovered. The technique is cost effective and allows for (a) excellent energy resolution—limited by the detector resolution rather than electronics; (b) dynamic time binning—rather than counting over predefined time bins, x-ray events are recorded as discretely timed events; (c) better noise rejection/pile up detection—achieved by fitting using the full information of the time history and known pulse shape from the amplifier; and (d) simple hardware implementation. The measured HXR energy flux is coupled to the Fokker–Planck code CQL3D to derive the electron distribution function for the fast electrons and infer the diffusion coefficient. The diagnostic has been used to measure diffusion coefficient on MST during improved confinement plasmas and measurements of radial diffusion of electron Bernstein wave (EBW) heated fast electrons are planned. © 2003 American Institute of Physics. [DOI: 10.1063/1.1535244]

I. INTRODUCTION

Recent measurements of the HXR flux caused by electron–ion bremsstrahlung emission in the core of MST using a single channel cadmium zinc telluride (CdZnTe) solid state detector indicates that energetic particles are confined during plasmas with edge current drive. Transport in reversed field pinch (RFP) plasmas has historically been dominated by magnetic stochastic processes: the radial magnetic field associated with resistive tearing modes causes field lines to wander stochastically preventing the formation of closed flux surfaces. Particles transport energy and lose confinement by flowing along the field lines, with the most energetic particles having the worst confinement.¹ Recent advances in understanding of the role of the current profile in the generation of the tearing modes, and subsequent current profile control experiments using pulsed poloidal current drive (PPCD), have improved confinement tenfold in the MST.^{2,3} The PPCD reduces the magnetic tearing mode amplitude by self-consistently replacing the current normally driven by an electric field generated by the correlation of velocity fluctuations with the tearing modes. In this article we describe a 16-channel array which extends previous x-ray measurements to simultaneous integrated line of sight profile measurements of the HXR flux. The diagnostic uses direct digitization which allows for more sophisticated software techniques to analyze the data after the discharge. This gives improved pile-up and noise handling since more information than just the height of pulse is recorded. It also allows more flexible time, energy binning of x-ray events. These measure-

ments are coupled to the Fokker–Planck code CQL3D to constrain the fast electron distribution and therefore its diffusion coefficient as a function of radius and energy.

II. DESCRIPTION OF DIAGNOSTIC

Following the work of Peysson,⁴ the diagnostic consists of 16 room temperature CdZnTe solid state detectors with active area 10 mm×10 mm×2 mm. Each detector is individually connected to any one of 17 available chords though a poloidal intersection of the MST. Figure 1 shows the lines of sight along, with an image of a solid state CdZnTe detector. Each chord has a 0.4 mm aluminum vacuum break which filters out the low energy (≤ 10 keV) x rays. The viewing solid angle is defined by the port holes in the MST vessel which are 31.75 mm diam and range between 180 and 320 mm distance from the detector depending on radial position. The collimated solid angle can be easily adjusted to ensure pile up fraction is kept to an acceptable level by directly mounting standard optical tube as spacer outside of the vacuum between the detector and the vacuum break. The current amplifiers are built into the housing of the detector itself, which has dimensions 20 mm×20 mm×50 mm. The raw signal is sent through a shaping amplifier which produces Gaussian pulses with 2 μ s half-width, with amplitude proportional to the x-ray energy. Conventionally signal at this stage is sent to a pulse height analyzer with predefined energy bins, and x rays falling within a given bin are then counted using a scalar counter. The pulse length of MST discharges is typically <60 ms, and the improved confine-

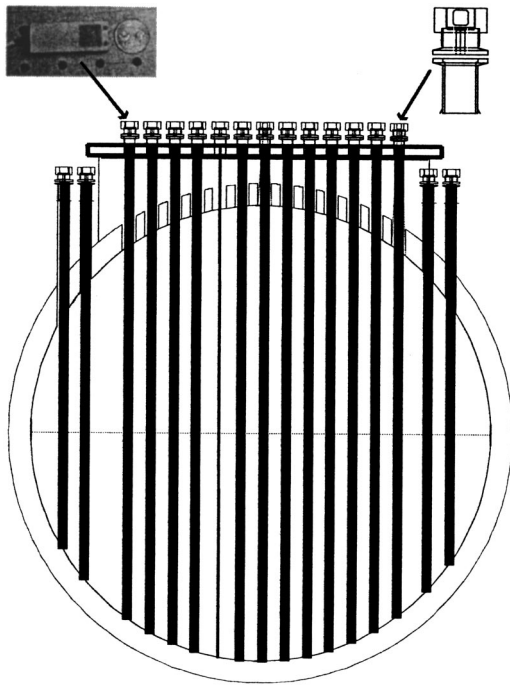


FIG. 1. Poloidal cross section of viewing chords. Actual detector shown top left.

ment periods during PPCD are ~ 10 ms. This makes direct digitization of the signal attractive. The ADC must be fast enough to capture the $2 \mu\text{s}$ Gaussian pulse and have enough memory to digitize most of the discharge. We have chosen a VME bus system with 2×8 channel, 12-bit, 10 MHz simultaneous sampling ADCs with 0.5 M samples storage per channel. This allows ~ 52 ms digitization period at the fastest sampling speed, although slower sampling speeds are acceptable at the expense of energy resolution. The 12-bit resolution of the ADC means that energy resolution is defined by the detector, which is $\sim 5\%$ of the incident photon energy. The 10 MHz digitization rate allows 20 points per Gaussian pulse. The width of the Gaussian pulse from the shaping amplifier defines the baseline counting rate, which is therefore ~ 500 kcps before pile-up, although with double Gaussian fitting closer spaced pulses can be resolved allowing a burst counting rate up to ~ 1000 kcps. The outputs from the shaping amplifier are simply connected to the ADC boards. The crate controller is a single board computer mounted in the VME crate. The computer stores the ~ 12 MB of raw data per discharge locally. Processed data (10s of kB) is sent to the main MST data system.

III. DATA DURING PPCD

Figure 2 shows raw data collected from a single channel of the HXR array during the application of PPCD during a 400 kA MST plasma. The insert shows a sample 0.1 ms period. X-ray events are seen as Gaussian pulses after the shaping amplifier. After the discharge, this raw data is processed on the VME computer: events are identified using a chosen trigger level and each event is fitted with a Gaussian function using the known half width of the pulse. This leaves three fitting parameters: the time stamp, the amplitude and

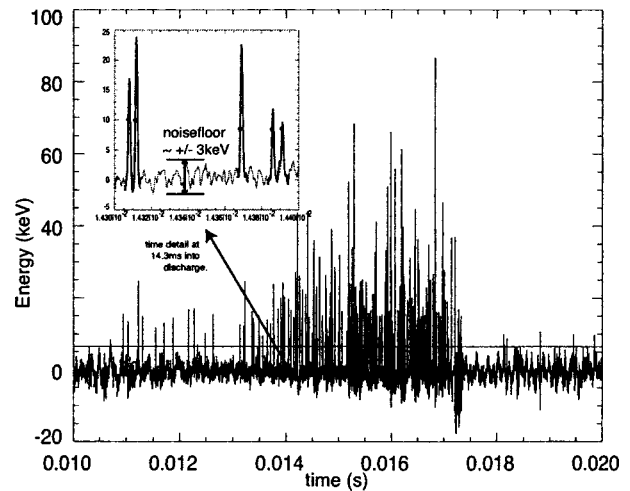


FIG. 2. Raw data of PPCD period with blow-up in time showing Gaussian pulses from the shaping amplifier.

the baseline shift. Any fits with too high χ^2 are then fitted with a double Gaussian. Events with still too high χ^2 are disregarded as either unsalvageable pile-up events or random noise. The fraction of events flagged as double Gaussian or pile-up is monitored and can be set according to the balance of higher bandwidth vs pileup fraction. At the end of the fitting procedure the HXR flux is stored as an array of precisely timed x-ray events for each line of sight, with a current uncertainty in time stamp of $\lesssim 1 \mu\text{s}$.

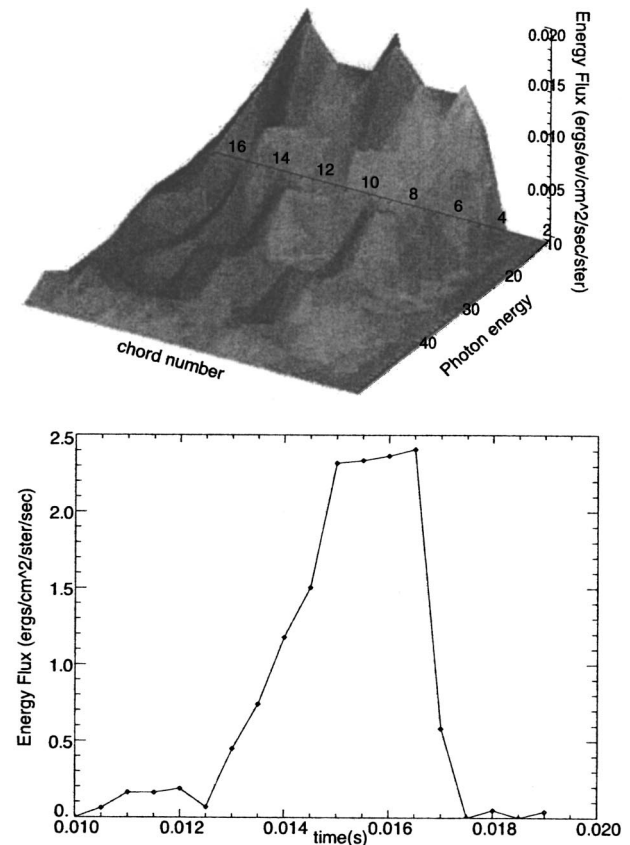


FIG. 3. (Top) Energy flux per chord vs energy at the end of PPCD (from 15.5 ms to 17 ms). (Bottom) The same data is rebinned to show the energy flux from photons greater than 10 keV. These data are sampled at 0.5 ms.

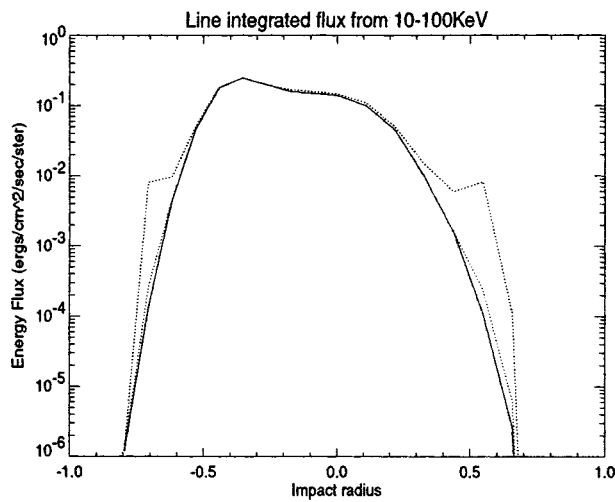


FIG. 4. HXR flux from PPCD and EBW heated plasmas.

The data can be histogrammed in any convenient manner and correlation analysis with other plasma diagnostics is a possibility; for example, the change in confinement time at the end of a PPCD enhanced confinement period.

Figure 3 shows how the timed x-ray events can be flexibly binned: the top graph shows processed profile data from a 1.5 ms period near the end of the PPCD enhanced confinement. The XR flux is normalized to a machine independent format which is compatible with CQL3D. The line of sight integral of the chords shown are plotted vs photon energy. The lower graph shows the same data but with all the x rays higher than 10 keV binned into one high resolution (0.5 ms) time history. The x-ray flux goes to zero in ~ 0.5 ms (less than a standard plasma confinement time) as the PPCD period ends.

IV. COUPLING TO FOKKER-PLANCK CODE CQL3D

The coupling of measured HXR flux to the Fokker-Planck simulation code CQL3D is an integral part of this

diagnostic. The CQL3D is multispecies, toroidal, fully relativistic radial transport code.⁵ It uses the measured plasma equilibrium with measured temperature and density profiles to calculate the spatial and temporal distribution function for both the electrons and ions. CQL3D includes a highly benchmarked bremsstrahlung diagnostic calculation. The line of sight integrals measured by the x-ray array are computed in CQL3D for direct comparison.

The primary free variable input to the code is the diffusion coefficient as a function of radius and energy. The coefficient is modified until the Ohmic input power (sensitive to the bulk electron diffusion) and HXR flux (sensitive to the energetic electron diffusion) agree with the measured values. As a minimum, the fact that x rays are detected during PPCD plasmas shows that energetic electrons are confined since it takes ~ 3 ms to accelerate bulk electrons to >50 keV. Hence the measured HXR flux is used to constrain the energetic electron population through the specification of the diffusion coefficient. Future applications of the diagnostic will be to directly measure the radial diffusion of energetic electrons heated by electron Bernstein waves in PPCD plasmas. Figure 4 shows calculations of 200 kA PPCD and 200 kA EBW heated PPCD plasmas. Experiments with EBW heating will be used to measure the electron radial diffusion during PPCD and possibly standard plasmas.

ACKNOWLEDGMENTS

The authors would like to thank Y. Peysson and L. Delpéch. This work was funded by the U.S. Department of Energy.

¹A. B. Rechester and M. N. Rosenbluth, Phys. Rev. Lett. **40**, 38 (1978).

²Chapman Brett *et al.*, Phys. Rev. Lett. **87**, 205001 (2001).

³C. R. Sovinec and S. C. Prager, Nucl. Fusion **39**, 777 (1999).

⁴Y. Peysson and F. Imbeaux, Rev. Sci. Instrum. **70**, 3987 (1999).

⁵R. W. Harvey, Cql3d, GA report No. GA-A20978, 1992.